

Large-Scale Synthesis of Single-Crystalline Perovskite Nanostructures

Yuanbing Mao,[†] Sarbajit Banerjee,[†] and Stanislaus S. Wong^{*,†,‡}

Department of Chemistry, State University of New York at Stony Brook, Stony Brook, New York 11794-3400, and
Materials and Chemical Sciences Department, Brookhaven National Laboratory, Building 480,
Upton, New York 11973

Received August 28, 2003; E-mail: sswong@notes.cc.sunysb.edu; sswong@bnl.gov

Nanoscale structures, such as nanoparticles, nanorods, nanowires, nanocubes, and nanotubes, have attracted extensive synthetic attention as a result of their novel size-dependent properties.¹ However, part of the challenge of developing practical nanoscale devices for a variety of applications is the ability to synthesize and characterize these nanostructures to rationally exploit their nanoscale optical, electronic, thermal, and mechanical properties. Strategies for the preparation of 1-D nanowires include formation from a confined alloy droplet, as described by the vapor–liquid–solid (VLS) growth mechanism, the kinetic control of growth through the use of capping reagents, the generation through a *chimie douce* solution chemical methodology, and the use of template-inspired methodologies.^{1,2} Comparatively little work has been performed on the fabrication of technologically important ternary perovskite transition metal oxide nanowires, which has hindered detailed experimental investigations on the size-dependent properties of these oxide materials.³ Developing approaches to prepare and scale up new synthetic formulations of these perovskite oxides has been the recent focus of our efforts.⁴

Ternary transition metal oxides, including BaTiO₃ and SrTiO₃, with a perovskite structure, are noteworthy for their exceptional dielectric, piezoelectric, electrostrictive, and electrooptic properties with corresponding electronics applications, including as electro-mechanical devices, transducers, capacitors, actuators, high-k dielectrics, dynamic random access memory, field-effect transistors, and logic circuitry.⁵ Previous work in synthesizing these materials has involved a number of different routes.^{3,4,6} While all of these methods are based on solution processes, they yield relatively small quantities of the desired nanostructures, and furthermore, in most cases, extremely toxic and unstable organometallic precursors are employed. Thus, the development of gram-scale and environmentally friendly synthetic methods with reproducible shape control is of paramount importance if the full potential of these materials is to be realized. To this end, we propose here a large-scale and facile solid-state reaction as a means of preparing single-crystalline BaTiO₃ and SrTiO₃ nanostructures in a NaCl medium at 820 °C in the presence of a nonionic surfactant.

In a typical synthesis, barium or strontium oxalate (depending on the desired nanostructure), TiO₂ (anatase), NaCl, and NP-9 (nonylphenyl ether) were mixed (molar ratio 1:1:20:3), ground for 25 min, and finally sonicated for 5 min. The mixture was then placed in a quartz crucible, inserted into a quartz tube, annealed at 820 °C for 3.5 h, and subsequently cooled to room temperature. Samples were collected, washed several times with distilled water, and dried at 120 °C overnight in a drying oven. We can easily and routinely scale up this process to produce grams of single-crystalline BaTiO₃ and SrTiO₃ nanomaterials.

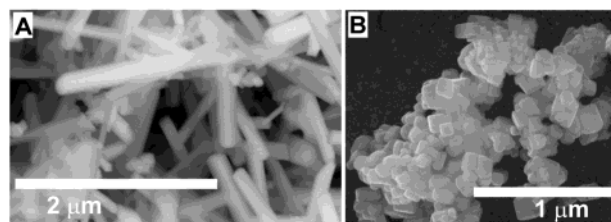


Figure 1. Scanning electron microscopy (SEM) images of as-prepared (A) BaTiO₃ nanowires and (B) SrTiO₃ nanocubes.

The purity and crystallinity of the as-prepared samples were examined using powder XRD (SI Figure S1). Very few if any impurity peaks are present. The peaks in Figure S1a can be indexed to the cubic lattice [space group: *Pm3m*] of BaTiO₃, and the calculated lattice constant is $a = 4.003 \text{ \AA}$, a value in good agreement with literature results ($a = 4.031 \text{ \AA}$, JCPDS no. 31-0174). Similarly, the peaks in Figure S1b can be indexed to a pure cubic phase of SrTiO₃ with a lattice constant $a = 3.884 \text{ \AA}$, compatible with the literature value of $a = 3.905 \text{ \AA}$ (JCPDS no. 73-0661).

Figure 1 shows SEM images of the as-prepared BaTiO₃ and SrTiO₃ products. From Figure 1A, it is evident that the BaTiO₃ product mainly consists of straight, smooth, and crystalline wire-like structures with relatively few particles. From the TEM results (Figure S2a), the nanowires are $\sim 50\text{--}80 \text{ nm}$ in diameter, and their lengths range from $1.5 \text{ }\mu\text{m}$ to even longer than $10 \text{ }\mu\text{m}$. SrTiO₃ nanostructures, analogously prepared, were revealed by SEM (Figure 1B) and TEM (Figure S2b) to consist exclusively of nanocubes with an edge length of $80 \pm 10 \text{ nm}$. It is evident that there is some degree of aggregation and clumping in these wires/cubes.

Images in A and B of Figure 2 represent the HRTEM images of the center region of one of the BaTiO₃ nanowires. While a thin amorphous layer can be found on the outer nanowire surface, the images clearly show that BaTiO₃ nanowires are uniform and homogeneous and that the 2-D lattice fringes illustrate that the nanowire is single crystalline with no defects or dislocations. EDS analysis (Figure 2C) from different positions along the nanowires shows that the chemical signatures of the nanowires are identical within experimental accuracy and that the nanowires are essentially composed of the elements Ba, Ti, and O. Moreover, the SAED patterns taken from different positions along the same nanowires are also identical within experimental accuracy, and the particular SAED pattern, shown here as an inset to Figure 2B, can be indexed to the reflection of a cubic BaTiO₃ structure with a lattice parameter, $a = 4.024 \text{ \AA}$, which is also consistent with the XRD data. The SAED pattern further validated that the observed BaTiO₃ nanowires are single crystalline. Furthermore, the tips of as-prepared BaTiO₃ nanowires (Figure 2, D and E) are smooth and hemispherical.

Figure 3A shows that the SrTiO₃ nanocube is effectively square in shape. Moreover, the 2-D lattice fringes (Figure 3B) illustrate

[†] State University of New York at Stony Brook.

[‡] Brookhaven National Laboratory.

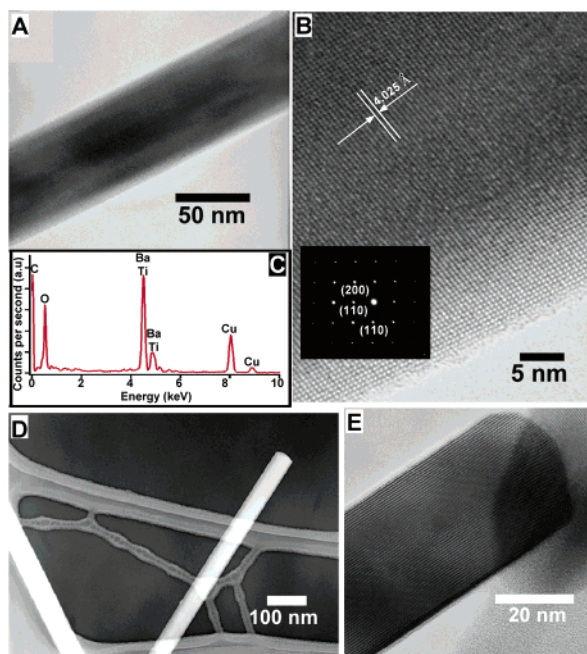


Figure 2. (A) Typical TEM micrograph of the BaTiO₃ nanowire. (B) High-resolution TEM (HRTEM) image of a portion of the nanowire in (A). Inset of (B) is the selected area electron diffraction (SAED) pattern of a BaTiO₃ nanowire. (C) Energy-dispersive X-ray spectroscopy (EDS) of the as-prepared BaTiO₃ nanowires. The Cu and C peaks originate from the TEM grid. (D) TEM image and (E) HRTEM image of representative tips of the as-prepared BaTiO₃ nanowires.

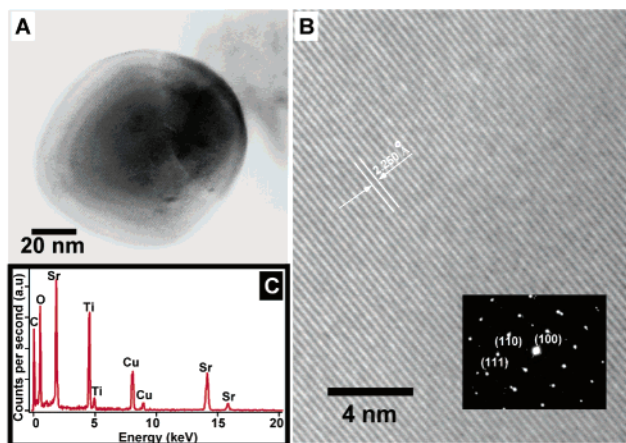


Figure 3. (A) TEM micrograph of an individual SrTiO₃ nanocube. (B) HRTEM image of (A), showing the crystal lattices, corresponding to the cubic phase. Inset of (B) is the corresponding SAED pattern of the as-synthesized SrTiO₃ nanocubes. (C) EDS analysis of the SrTiO₃ nanocubes. The Cu and C peaks originate from the TEM grid.

that the nanocubes are single crystalline with no defects or dislocations. Interplanar spacings are ~ 2.250 Å. EDS data indicate that these cubes are composed of Sr, Ti, and O (Figure 3C). The SAED pattern (inset to Figure 3B) can be indexed to the reflection of a cubic SrTiO₃ structure with $a = 3.885$ Å.

It is noteworthy that the use of different precursors, such as oxides and chlorides, as opposed to oxalates, produces neither phase-pure titanates nor even nanostructures. Moreover, even a slight change of reaction conditions, such as at a slightly lower temperature, i.e., 810 °C, results in a lack of phase-pure titanates.

Our experimental results demonstrate that maintaining identical experimental conditions, with the exception of the metal precursor (i.e. either Ba- or Sr-based) used, results in the production of different shapes of perovskite nanostructures. Although the funda-

mental basis of shape selectivity for this system is not as yet known, it is likely that wires and cubes are simply kinetically dissimilar, morphological manifestations of the same underlying growth mechanism, involving the formation of initial nuclei of the cubic form.⁷ The shape of a nanocrystal may also be determined by the relative specific surface energies associated with the facets of the crystal. In addition, the preferential adsorption of molecules and ions, such as chloride, to different crystal faces likely directs the growth of nanoparticles to their ultimate product morphology by controlling the growth rates along the different crystal faces.^{2b,8} In fact, if NaCl is removed from the synthesis of BaTiO₃ nanowires, the product is randomly particulate in shape distribution. It makes little difference in the SrTiO₃ synthesis whether NaCl or surfactant is present in the reaction mixture. Moreover, if the initial barium or strontium precursor is omitted altogether, identical experimental protocols all yield cubes, consisting of a mixture of anatase and rutile.

In summary, single-crystalline BaTiO₃ nanowires and SrTiO₃ nanocubes have been prepared with a novel and simple one-step solid-state chemical reaction in the presence of NaCl and a nonionic surfactant. Because of the simplicity and generalizability of the approach used, it is anticipated that this methodology can be expanded to the large-scale synthesis (gram quantity) of other important ferroelectric systems at the nanoscale, such as PbTiO₃ and BaZrO₃. Future work involves the nanoscale investigation of ferroelectricity, piezoelectricity, and paraelectricity as well as mechanistic studies of nanowire/nanocube formation for the purpose of synthetic optimization.

Acknowledgment. Support of this work was provided through startup funds from SUNY Stony Brook and BNL, as well as through the donors of the PRF, administered by the ACS. We also thank Dr. J. Quinn (Stony Brook) and Dr. J. Huang (Boston College) for SEM/TEM work and HRTEM analysis, respectively.

Supporting Information Available: XRD patterns and TEM images; characterization conditions are described (PDF). This material is available free of charge via the Internet at <http://pubs.acs.org>.

References

- (1) (a) Hu, J.; Odom, T. W.; Lieber, C. M. *Acc. Chem. Res.* **1999**, *32*, 435. (b) Patzke, G. R.; Krumeich, F.; Nesper, R. *Angew. Chem., Int. Ed.* **2002**, *41*, 2446. (c) Xia, Y.; Yang, P.; Sun, Y.; Wu, Y.; Mayers, B.; Gates, B.; Yin, Y.; Kim, F.; Yan, H. *Adv. Mater.* **2003**, *15*, 353. (d) Rao, C. N. R.; Nath, M. *Dalton Trans.* **2003**, 1.
- (2) (a) Wu, Y.; Yan, H.; Huang, M.; Messer, B.; Song, J. H.; Yang, P. *Chem. Eur. J.* **2002**, *8*, 1260. (b) Pantes, V. F.; Krishnan, K. M.; Alivisatos, A. P. *Science* **2001**, *291*, 2115. (c) Song, J. H.; Messer, B.; Wu, Y.; Kind, H.; Yang, P. *J. Am. Chem. Soc.* **2001**, *123*, 9714. (d) Mo, M.; Zeng, J.; Liu, X.; Yu, W.; Zhang, S.; Qian, Y. *Adv. Mater.* **2002**, *14*, 1658. (e) Mbindyo, J. K. N.; Mallouk, T. E.; Mattzela, J. B.; Kratochvilova, I.; Razavi, B.; Jackson, T. N.; Mayer, T. S. *J. Am. Chem. Soc.* **2002**, *124*, 4020.
- (3) Urban, J. J.; Spanier, J. E.; Ouyang, L.; Yun, W. S.; Park, H. *Adv. Mater.* **2003**, *15*, 423.
- (4) Mao, Y.; Banerjee, S.; Wong, S. S. *Chem. Commun.* **2003**, 408.
- (5) (a) Hill, N. A. *J. Phys. Chem. B* **2000**, *104*, 6694. (b) Schrott, A. G.; Misewich, J. A.; Nagarajan, V.; Ramesh, R. *Appl. Phys. Lett.* **2003**, *82*, 4770. (c) Tao, S.; Irvine, J. T. S. *Nat. Mater.* **2003**, *2*, 320.
- (6) (a) Liu, C.; Zou, B.; Rondinone, A. J.; Zhang, Z. J. *J. Am. Chem. Soc.* **2001**, *123*, 4344. (b) O'Brien, S.; Brus, L.; Murray, C. B. *J. Am. Chem. Soc.* **2001**, *123*, 12085. (c) Hernandez, B. A.; Chang, K.-S.; Fisher, E. R.; Dorhout, P. K. *Chem. Mater.* **2002**, *14*, 480.
- (7) Wang, Z. L. *J. Phys. Chem. B* **2000**, *104*, 1153.
- (8) (a) Murphy, C. J. *Science* **2002**, *298*, 2139. (b) Filankembo, A.; Giorgio, S.; Lisiecki, I.; Pileni, M. P. *J. Phys. Chem. B* **2003**, *107*, 7492.

JA038192W